Quantum-Resolved Investigations of Flux Dynamics: Collective and Single Vortex Effects

S. T. Stoddart and S. J. Bending
School of Physics, University of Bath, Claverton Down, Bath, BA2 7AY, United Kingdom

A. K. Geim and M. Henini
Department of Physics, University of Nottingham, University Park, Nottingham, NG7 2RD, United Kingdom
(Received 9 August 1993)

The dynamics of flux vortices in Pb films has been investigated with single fluxon resolution. With increasing magnetic field, there is a crossover from a region where single vortex effects dominate to one where vortex motion becomes correlated. We have measured the flux bundle correlation radius directly and tracked single vortices or correlated bundles as they moved under the action of an applied dc current or in response to a change in temperature. The signatures of flux flow and flux creep have been identified, enabling us to determine the pinning force at individual pinning sites.

PACS numbers: 74.60.Ge, 72.20.My, 74.25.Ha, 74.76.Db

Since the discovery of high-temperature superconductors, there has been renewed interest in the properties of magnetic flux vortices in the mixed state [1] and the crossover between single vortex and collective pinning regimes, in particular, is being actively investigated [2]. The techniques which are commonly applied to probe vortex dynamics (e.g., transport and magnetization measurements) are indirect and results on bulk samples are dependent on theoretical models [3]. For example, during flux flow or flux creep in type II superconductors, the flux vortices are believed to move in correlated bundles of several fluxons, yet, until now, there has been no direct measurement of the bundle diameter. In addition the interaction of flux vortices with pinning centers dominates transport properties, yet little is known about the pinning force at individual pinning sites. There are a number of methods for examining flux vortices on a microscopic scale, for example, flux decoration [4], imaging in Josephson junctions [5] and SQUIDs [6], scanning tunneling microscopy [7], and electron holography [8]. However, each technique has its limitations and is often laborious to apply. In contrast, micron-sized Hall probes have many advantages for the investigation of both static and dynamic flux structures with high spatial resolution (<0.5 μm) over a broad temperature range (0–150 K) [9,10]. Hall probes have frequently been used by other authors to investigate flux structures in superconductors but rarely with such high spatial resolution and never in the way described here [11,12]. In this work we are able to probe single and collective vortex phenomena with fluxon resolution. We directly measure flux bundle correlation diameters and vortex pinning forces at individual pinning centers and study the interplay between pinning forces and intervortex interactions as the mean vortex spacing, Lorentz force, and temperature are varied. In addition we can estimate the distances vortices and vortex bundles move during displacements.

A high-mobility $GaAs/Al_{0.3}Ga_{0.7}As$ two-dimensional electron gas (2DEG) [$n_{2D}=2.9\times10^{15}$ m^{-2}, μ(7.5 K) $=81$ m^{2}V^{-1}s^{-1}] was wet chemically etched into Hall probes with characteristic linewidths ranging from 0.5 up to 8 μm. Neither the electron concentration nor the mobility changed significantly over the temperature range covered by the experiments. In practice the most useful detectors were found to be those of linewidth 2 μm and an active area of 4 μm^2 which displayed very low noise and high sensitivity ($\rho_{xy}\approx 1$ Ω/Φ_0). The spatial separation of Hall probe and superconductor leads to slight broadening of the flux vortices at the detector, but our calculations show [10] that fluxons are well resolved at all the applied magnetic fields used except very close to T_c (7.2 K at $H=0$). The Hall probe is operated with a small 31 Hz ac current to eliminate tiny induced dc signals due to a flux transformerlike action when vortices move in the superconducting gate [13] and with our experimental setup it proved possible to detect amounts of flux smaller than $\frac{1}{100}$ of a flux quantum.

We chose to investigate Pb films since these show the largest peak vortex fields of all known superconducting materials and could easily be thermally evaporated onto GaAs at room temperature. The 20-μm-wide Pb films were 200 nm thick and, as shown in previous decoration experiments [14], show type II behavior with $\mu_0 H_{c2}(T=0)$ estimated to be 0.10 T. The films were granular, had a resistivity of 8.7×10^{-9} Ω m at 8 K, and were in the clean limit ($l_e \sim 2\xi_0$). Since the films were much thicker than the low-temperature penetration depth [$d>5\lambda(0)$] bulk expressions have been used to describe the superconducting properties. Gold wires were attached to the Pb films using silver epoxy so that a transport current could be applied and a constant shunt of 4–5 times the normal state resistance of the film was connected in parallel to protect against thermal runaway. The GaAs substrate bearing the Hall bar structure and Pb film was epoxied onto an alumina chip carrier which was, in turn, glued onto a temperature-controlled copper sample holder. The sample temperature could be stabilized to within 1 mK using He exchange gas and a commercial

0031-9007/93/71(23)/3854(4)$06.00

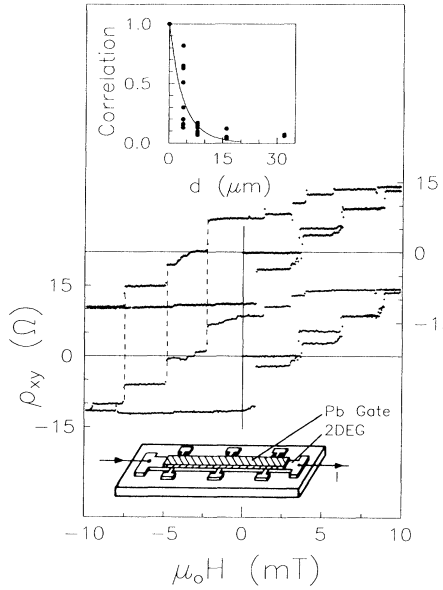

FIG. 1. Hall resistivity measured simultaneously at two Pb-gated detectors with 4 μm separation at 4.3 K. A resistivity of 1 Ω corresponds to a single flux line threading the 2 μm$\times$2 μm detector. The lower inset shows a sketch of the sample. The upper inset plots the correlation coefficient at various contact separations.

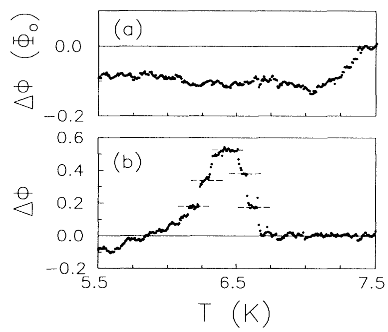

FIG. 2. (a) The change in flux ($\Delta\phi$) threading a Hall probe as a function of temperature at an applied field of 0.5 mT. (b) The same measurement at an applied field of 10 mT.

temperature controller. The modest fields applied during the experiments were provided by a copper solenoid.

During our measurements we could vary the magnetic field, temperature, and supercurrent in the Pb film at will, which enabled three distinct types of experiments to be performed. In the first of these, the film was cooled in zero field to the desired temperature and the applied magnetic field swept around a cycle while the Hall voltage was recorded simultaneously at two pairs of contacts of known separation (see inset to Fig. 1). A typical result for probes 4 μm apart is shown in Fig. 1. Each of the abrupt steps corresponds to the entry of a number of vortices into the area of film above a given probe. Note that a large fraction of the steps occur simultaneously, implying that the same flux bundle extends over both pairs of contacts. By counting the number of simultaneous events, and dividing by the total number of steps at both contacts, we obtain a correlation coefficient c $(0<c<1)$, which is plotted in an inset to Fig. 1. Assuming that flux bundles are rigid cylinders of radius r distributed randomly along the length of the Pb film, we have developed a simple model for the correlation coefficient. If all bundles have the same radius, we calculate from simple geometrical considerations that $c(r,d)=1-d/(2r+w)$, where d is the probe separation and w the linewidth of the Hall probe. In reality the flux bundles will not have a fixed radius and, assuming a Poisson distribution of radii with mean radius r_0, $\rho(r,r_0)=(1/r_0)\exp(-r/r_0)$ we calculate $\langle c(r_0,d)\rangle=\int_0^\infty c(r,d)\rho(r,r_0)dr$. The solid line in the inset to Fig. 1 is a fit to this expression with $r_0=2.5$ μm, corresponding to a 5 μm bundle diameter at 4.3 K. This compares favorably with theoretical estimates of the collective pinning correlation radius due to Larkin and Ovchinnikov [3] $[R_c=(c_{66}/f_p n^{0.5})(2\Phi_0/\sqrt{3}B)^{1/2}\sim 1.25$ μm at 5 mT] where we have assumed that the density of pinning sites n is the same as the density of Pb grains, pinning forces f_p are taken from experiments described below, and the flux lattice elastic modulus c_{66} is estimated from magnetization measurements on large samples. At higher temperatures $(T<T_c)$ we observe a reduction in the bundle correlation radius consistent with the expected softening of c_{66}.

In a second type of experiment [5] the film was cooled from above T_c to 4.5 K in an applied field. The field was held constant while the temperature was slowly increased and the Hall voltage at a single probe monitored (Fig. 2). In previous experiments on macroscopic probes with comparable carrier densities [15], we have shown that the Hall voltage depends only on the net flux threading the active area, *not* on its spatial distribution. At the microscopic level this may no longer be true due to the absence of ensemble averaging, but based on many field-cooling experiments on micron-sized probes, we infer that the Hall voltage only varies by $<\pm 10\%$ as the position of a vortex is changed within the active area and any variations in Fig. 2 correspond to vortices moving at the edge of the sensor. Figure 2(a) shows data at the small applied field of 0.5 mT where on average there is one vortex threading the active area of the detector and the changes in measured flux are smooth and continuous. This reflects small movements of a single vortex towards or away from the edge of the probe due to changes in the pinning potential arising from the temperature-dependent superconducting parameters [e.g., $\lambda(T)$]. Note that these fluctuations exceed the instrumental noise level which can be estimated from the spread of data points for $T>T_c$ when the Hall probe sees a constant, uniform field. At 10 mT [Fig. 2(b)], the vortices are closer together and intervortex interactions become important. In this figure, we

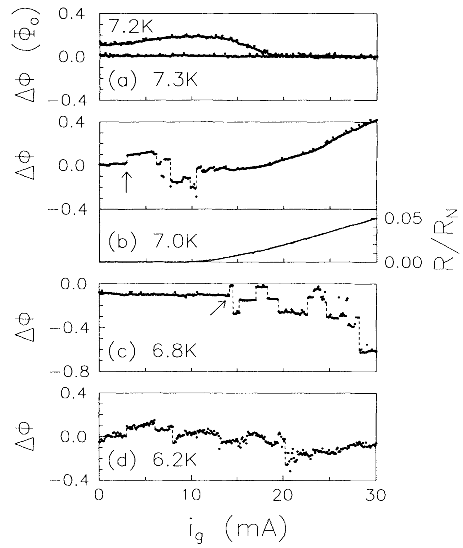

FIG. 3. (a)–(c) The change in flux ($\Delta\phi$) threading a Hall probe as a function of gate current I_g in an applied field of 1 mT at various temperatures and (d) in 10 mT at 6.2 K. The arrows indicate the feature used to build Fig. 4. Included in (b) is the I-R curve of the Pb gate normalized by the resistance at 8 K.

see that the vortices suddenly rearrange themselves under the competing influences of pinning forces and intervortex interactions, causing the discrete steps in the Hall voltage. (Note that at 10 mT, T_c is reduced to 6.7 K.) Clearly at these larger fields the intervortex interaction becomes so large that a small cluster of vortices actually moves between different minima of the collective pinning potential at certain threshold temperatures. The mean spacing of the vortices at 10 mT is 490 nm and from standard expressions [13] $[f_{12}(r_{12}) \cong (\Phi_0^2/2\pi\mu_0\lambda^2)(\pi/2r_{12}\lambda)^{1/2}\exp(-r_{12}/\lambda)]$ we estimate the intervortex force at 6.5 K to be $\sim 10^{-6}$ N m^{-1}. We note that this is comparable with the expected single vortex pinning force at this temperature as measured below, lending strength to the idea that competition between the two is important here. This sudden motion of vortex bundles must involve energy dissipation and represents a flux noise mechanism even in the absence of an applied supercurrent. Modeling a vortex as a cylinder of uniformly distributed flux of radius $\lambda(T)$, the Hall voltage can be considered to measure the area of intersection between this cylinder and the active part of the Hall probe (assumed to be defined by the square intersection of voltage and current leads). Considering the two extreme cases of a cylinder either whose circumference or whose axis is just touching the edge of the active area, a change in Hall voltage can be converted into a lateral displacement of a flux vortex. In the case of the flux bundle imaged in Fig. 2(b), we assume that we are observing one critical vortex near the probe perimeter and that elastic distortions of the bundle are small compared to the bundle displacement. This allows us to estimate that the correlated vortex regions are typically moving distances of 20–40 nm during jumps.

The final class of experiments was performed with a dc supercurrent flowing through the Pb film at constant temperature and magnetic field. The samples were initially field cooled from above T_c to the target temperature with no current flowing in the film, whereupon the dc current was slowly ramped up to 30 mA while the Hall voltage at a single probe was monitored. Examples of ramps at different temperatures are shown in Figs. 3(a)–3(c) for a small applied field of 1 mT when vortices can be considered to be well isolated. Note that at $T=7.3$ K ($T > T_c$) the Hall voltage is constant as one would expect. The Hall voltage is also constant when the current density in the film $J \ll J_c$. Above about 6 K there is a threshold current where there is a sudden discontinuous change in Hall voltage and an irregular sequence of square steps is observed as the current is increased. At still higher temperatures ($T < T_c$) these steps give way to a smooth *upwards* curve indicating that the net flux threading the probe is continuously *increasing*. Just below T_c, only the smooth curve is observed, which at a certain current rolls off to yield the normal state behavior. By comparing the behavior of the Hall voltage with four-point dc I-V measurements performed directly on the Pb film [Fig. 3(c)], we make the following identifications: The abrupt steplike structure represents the onset of flux creep when individual vortices hop between pinning sites, while the smooth upwards curvature corresponds to the onset of flux flow. In the flux creep regime, assuming that the dc current in the film is uniformly distributed, it is possible to estimate the Lorentz force F_L on a vortex, $\mathbf{F}_L = \mathbf{J} \times \mathbf{\Phi}_0$ where J is the current density in the film and Φ_0 is the flux quantum. The threshold current at which the first step is observed (indicated by the arrows in Fig. 3) yields a Lorentz force equal to the pinning force for the vortex at that particular position. The pinning force at one specific site $f_p(T)$ has been compared to an empirical power law, $f_p(T) = f_p(0)(1 - T/T_c)^n$, in Fig. 4. We find that the parameter $f_p(0)$ varies from $(0.8\text{–}3)\times 10^{-6}$ N m^{-1} and the exponent n from 1.5–2 for different pinning sites. In Josephson junction experiments on 380-nm-thick Pb films, Li, Clem, and Finnemore [16] found $n \approx 1$ over a similar temperature range and rather smaller values of pinning force. This difference perhaps reflects differences in film thickness and quality. From scanning electron micrographs we see that our films are granular with a grain size of ~ 200 nm. In addition to there being increased electron scattering at the grain boundaries, there also appears to be a reduction in film thickness there, so it is highly likely they are the dominant pinning sites in our films. The wide spread in our measured values of n suggests that there is no generic temperature dependence for this mechanism; rather it depends on the microscopic details of the pinning site. Note that the points in Fig. 4 are a compilation of data for a specific pinning site gained from sweeps of I_g with T held

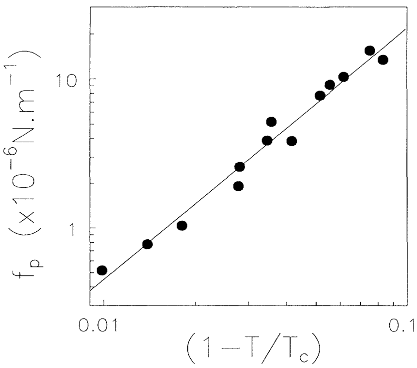

FIG. 4. Pinning force at one particular site in the Pb film plotted as a function of $(1-T/T_c)$. The straight line is a fit to an empirical form (see text).

constant as well as sweeps of T with I_g held constant at *both* 0.5 and 1 mT. The fact that the Hall voltage step used to obtain a pinning force is repeatable in size and direction for different temperatures and fields and yields data which fall on a single universal curve is clear evidence that a single pinning center is involved. Note that at 0.5 and 1 mT the mean vortex spacing is so large that intervortex interactions are negligible and there will be no collective pinning. Once again the height of the steps in Hall voltage implies that vortices are traveling ~20–40 nm during hops and we speculate that they are probably moving short distances along grain boundaries. In the flux flow regime bundles of vortices cross the detector extremely rapidly, individual vortices cannot be resolved, and an average voltage is measured. The upward trend to the Hall voltage in this regime is consistent with a vortex/antivortex nucleation mechanism of the critical current in these films whereby vortices and antivortices enter at opposite edges of the film, move towards the center under the influence of the Lorentz force, and annihilate each other. Because of the existence of an applied magnetic field, the annihilation point will be off center, and the probe, which is near the geometrical center of the film, will see an increased vortex density.

Figure 3(d) plots the change in flux threading the detector upon application of a gate current at 6.2 K in a 10 mT applied field. The apparent increase in noise in this figure is an instrumental artifact resulting from the subtraction of the background Hall voltage which is now 10 times larger. At this magnetic field the vortices are close enough that one would expect to observe collective effects and we note that the signal has now assumed a pronounced sawtoothlike profile. We interpret this as arising from smooth elastic distortions of correlated regions of flux vortices followed by sudden jumps when a local collective pinning force is exceeded. Indeed an analysis of the smoothly increasing sections of the data yields an elastic constant which is consistent with our earlier estimates if we assume correlated regions of ~4–10 vortices.

In conclusion, we have used 2 μm Hall probes to study the dynamics of vortices in 200 nm Pb films. Coincidence measurements have allowed a direct estimate of the correlation diameter of vortex bundles which is in reasonable agreement with theoretical estimates [3]. We have also been able to track single vortices and correlated bundles as they moved under the action of an applied dc current or in response to a change in temperature. The signatures of flux creep and flux flow have been identified, allowing pinning forces at individual pinning sites to be measured. Finally, we note that submicron Hall probes should be particularly useful in helping to understand the rich new phenomena observed in high-temperature superconductors.

This work was supported by SERC Grant No. GR/H23573 and Royal Society Research Grant No. 11552.

[1] For a review, see D. A. Huse, M. P. A. Fisher, and D. S. Fisher, Nature (London) **358**, 553 (1992).
[2] L. Krusin-Elbaum, L. Civale, V. M. Vinokur, and F. Holtzberg, Phys. Rev. Lett. **69**, 2280 (1992).
[3] P. W. Anderson and Y. B. Kim, Rev. Mod. Phys. **36**, 39 (1964); A. I. Larkin and Yu. N. Ovchinnikov, J. Low Temp. Phys. **34**, 409 (1979).
[4] H. Träuble and U. Essmann, J. Appl. Phys. **39**, 4052 (1968).
[5] S. C. Sanders, J. Sok, D. K. Finnemore, and Q. Li, Phys. Rev. B **47**, 8996 (1993).
[6] G. S. Park, C. E. Cunningham, B. Cabrera, and M. E. Huber, Phys. Rev. Lett. **68**, 1920 (1992).
[7] H. F. Hess *et al.*, Phys. Rev. Lett. **62**, 214 (1989).
[8] T. Matsuda *et al.*, Phys. Rev. Lett. **62**, 2519 (1989).
[9] S. T. Stoddart, H. I. Mutlu, A. K. Geim, and S. J. Bending, Phys. Rev. B **47**, 5146 (1993).
[10] S. J. Bending, K. von Klitzing, and K. Ploog, Phys. Rev. B **42**, 9859 (1990).
[11] T. Tamegai *et al.*, Phys. Rev. B **45**, 8201 (1992).
[12] A. M. Chang *et al.*, Appl. Phys. Lett. **61**, 1974 (1992).
[13] M. Tinkham, *Introduction to Superconductivity* (McGraw-Hill, New York, 1975).
[14] A. K. Geim, V. I. Falko, S. V. Dubonos, and I. V. Grigorieva, Solid State Commun. **82**, 831 (1992).
[15] A. K Geim, S. J. Bending, and I. V. Grigorieva, Phys. Rev. Lett. **69**, 2252 (1992).
[16] Q. Li, J. R. Clem, and D. K. Finnemore, Phys. Rev. B **43**, 12843 (1991).